
RISET
Geologi dan Pertambangan
Open access https://jrisetgeotam.lipi.go.id/index.php/jrisgeotam Geology and Mining Research
Riset Geologi dan Pertambangan (2023) Vol.33, No.2, 77–88, DOI: 10.55981/risetgeotam.2023.1257

Research article

Presupposition of slip plane using the 2D resistivity method with dipole-dipole array in Jahiang Village, Salawu District, Tasikmalaya Regency, West Java Province

Risky Martin Antosia[1], Fitri Pangaribuan[1], and Dadan Dani Wardhana[2]

[1]Geophysical Engineering Department, Faculty of Industrial Technology, Sumatera Institute of Technology, Indonesia.
[2]Research Center for Geological Disasters, National Research and Innovation Agency (BRIN), Indonesia.

Keywords:
Dipole-dipole array
Landslide
Resistivity
Slip plane
Salawu Tasikmalaya

Corresponding author:
Risky Martin Antosia
Email address: martin.antosia@tg.itera.ac.id

Article history
Received: 21 July 2023
Revised: 02 December 2023
Accepted: 20 December 2023

ABSTRACT

Landslide disasters frequently occur in Tasikmalaya Regency, with Salawu Village being at a medium to high ground movement vulnerability zone. Steep slopes and quite high rainfall dominate this area. This study aims to identify subsurface rock types and model the slip plane by applying the dipole-dipole configuration of the 2D geoelectrical method. The result can be used as a mitigation measure to minimize losses if a landslide disaster occurs. We measured the resistivity in five lines with spacing between electrodes of 5 m with a total length of 275 m. The data processing results indicate three classes of resistivity values: a resistivity value under 25 Ωm is interpreted as sandy clay, a value in the range of 20-105 Ωm as clayey/ tuffaceous sand, and a resistivity of more than 80 Ωm as volcanic breccia. The slip area is sandy clay with a slipping mass of clayey/ tuffaceous sand and volcanic breccia. Two of the surveyed lines have safety factor values less than 1.00 (the slope is approximately 40°, and the slip plane angle is between 33° and 35°), which means that the area has an unstable slope. The small safety factors should be a serious concern because landslides can occur at any time. Moreover, breccia rock is one of the landslide materials that would have a very destructive impact. To confirm the results of this study, in situ geomechanical tests are needed in this area.

INTRODUCTION

The movement of rocks in a vertical, horizontal, or inclined direction from their original position is called a landslide. Landslides often occur during the rainy season, when water seeps into the ground through rocks that can pass water (permeable) until the water is trapped in rocks that cannot pass water (impermeable). Then, the land on top of impermeable rocks will experience weathering, which over time will make the soil saturated with water, increasing soil weight. Subsequently, the slope becomes unstable that the hill will move to find a new balance, and then a landslide will occur (Darsono et al., 2012).

Based on the 2021 Indonesian Disaster Risk Index, Tasikmalaya Regency has a natural disaster index level of 186.51, which is classified as high, and the landslide risk index is 15.80, which is also ranked high (Adi et al., 2023). For example, the Tasikmalaya Regency Disaster Management Operations Control Center said that there were 374 natural disasters in 2022, of which 240 were landslides, with losses reaching 8 billion rupiah in 2022 (Miranti, 2022). Jahiang Village is one of the villages in Salawu District, Tasikmalaya Regency, West Java Province, where landslides occur frequently. The Center for Volcanology and Disaster Mitigation (PVMBG) said that Salawu District has the potential for medium to high-ground movement (Kompas, 2011). The medium ground movement susceptibility zone has a slope of 5% - 15% (8° - 26°), while the high movement susceptibility zone has a slope of 30% - 50% (57° - 119°). The last occurrences of landslides were recorded in 2017 (Azwar, 2017), 2019 (Muslim, 2019), and 2021 (Analisa global, 2021). In a previous study, Sarah & Daryono (2012) carried out engineering geological measurements to identify slow ground movement in Jahiang Village, Salawu District, Tasikmalaya Regency, using local topographic capture, geotechnical drilling, hand drills, cone penetration tests, and laboratory tests. The research obtained information on groundwater zones that influence slope movement, thus indicating that the area is an active landslide area.

One influential factor of a landslide is the slip plane or slip surface. The land or landslide area above this slip area is called landslide material. One method that can identify slip areas is the geoelectrical resistivity method. The resistivity geoelectric method can describe subsurface structures based on the electrical properties of rocks by injecting current into the subsurface with a current electrode and then measuring the potential difference with a potential electrode (Dentith & Mudge, 2014; Reynolds, 2011). Commonly, the method is employed for groundwater prospecting (Antosia, 2023a; Antosia & Ramdan, 2023d; Fatimah et al., 2021; Yuniardi et al., 2019) and geological assessment (Antosia et al., 2023b, 2023c). Furthermore, the technique can also be applied to identify landslide zones (Darsono et al., 2012; Putra et al., 2020; Taufiqurrohman et al., 2017) and analyze ground movement (Djakamihardja, 2008; Wakhidah et al., 2014). The landslide is a slow movement involving residual soil from soft to dense sandy clay, clayey to thick sand, and fresh to weathered breccia rock. The resistivity technique can roughly depict impermeable and porous layers among those rocks/layers.

The dipole-dipole array is generally used for mineral exploration (Arifin et al., 2019; Dewi et al., 2017) and cavity/void detection (Al-Oufi et al., 2012; Stevanato et al., 2019; Vargemezis et al., 2015). In this study, we applied the array because of its lateral sensitivity, particularly to boulder anomaly. Based on the previous explanation, the breccia rock can be found in the area. Therefore, with the implementation of the dipole-dipole configuration, we wanted to identify the possible boulder size of rocks. Such a layer can act as a slip plane or sliding rock mass. Furthermore, after the slip plane was approximated, the factor of safety was also be calculated.

GEOLOGICAL SETTINGS

This study is conducted in Jahiang Village, Salawu District, Tasikmalaya Regency, West Java Province. Geologically, Tasikmalaya Regency is in the formation of the Quaternary Volcanic Zone, Central Depression Zone, and Southern Mountain Zone. Tasikmalaya was previously known as *Tawang/ Galunggung*, meaning broad rice fields in Sundanese. After Mount Galunggung erupted, the *Tawang* area turned into a sand area, so this area's name was changed to Tasikmalaya, where "Tasik" means lake and "Malaya" means dunes in Sundanese. The Central Depression Zone is in the central part of Tasikmalaya Regency and has steep hilly topography separated by valleys, resulting in mountain folds (Intermontane depression) due to tectonic activity. The Southern Mountain Zone, which is dominated by highlands of limestone areas, stretches from Pelabuhan Ratu to Nusakambangan Island, where limestone caves can be found. This area indicates that it was once under the sea and uplifted by tectonic energy (Van Bemmelen, 1949).

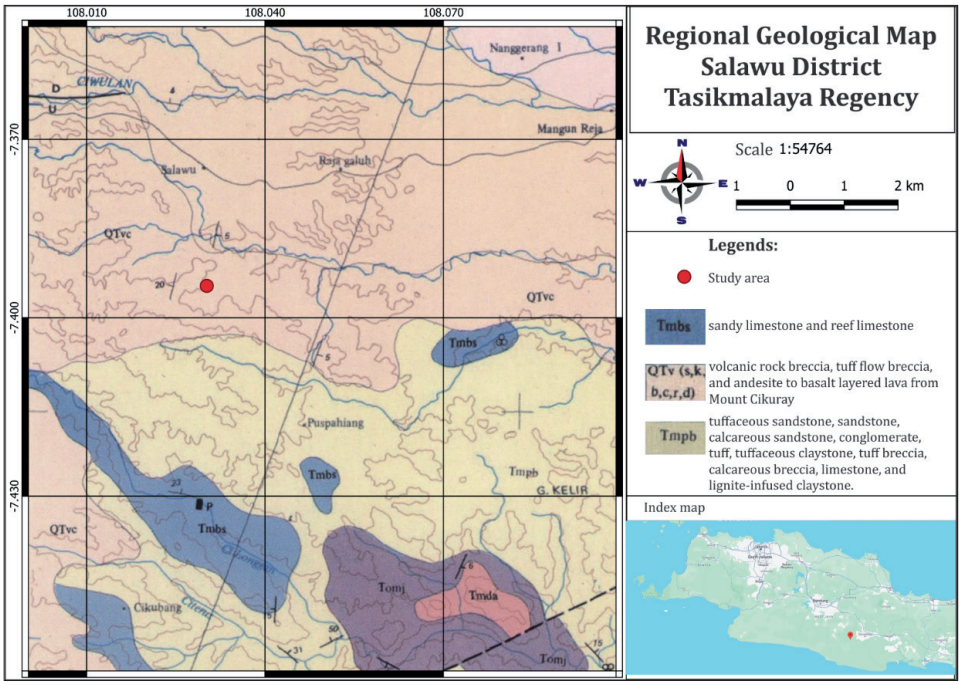

Figure 1. Geological map of the study area (modified from Budhitrisna, 2010).

Figure 1 indicates that Salawu District is dominated by rocks with the Tmbs, QTv, and Tmpb formations. The Tmbs Formation (Surajara member) consists of sandy and reef limestones. The QTvc formation (the product of old volcanoes) consists of volcanic breccia, tuff breccia, and lava with andesite to basalt composition from Mount Cikuray. The Tmpb Formation (span formation) consists of tuffaceous sandstone, sandstone, calcareous sandstone, conglomerate, tufa, tuffaceous claystone, tuff breccia, calcareous breccia, limestone, claystone, and lignite inserts (Budhitrisna, 2010). Geographically, the region is located on the boundary line 108°02'-108°03' East Longitude and 7°38'-7°41' South Latitude, with the size of the study area being about 300m ×× 300m. The location is hilly, with topography sloping to the northwest in general. Its slope ranges from 20° to 40° (Figure 2).

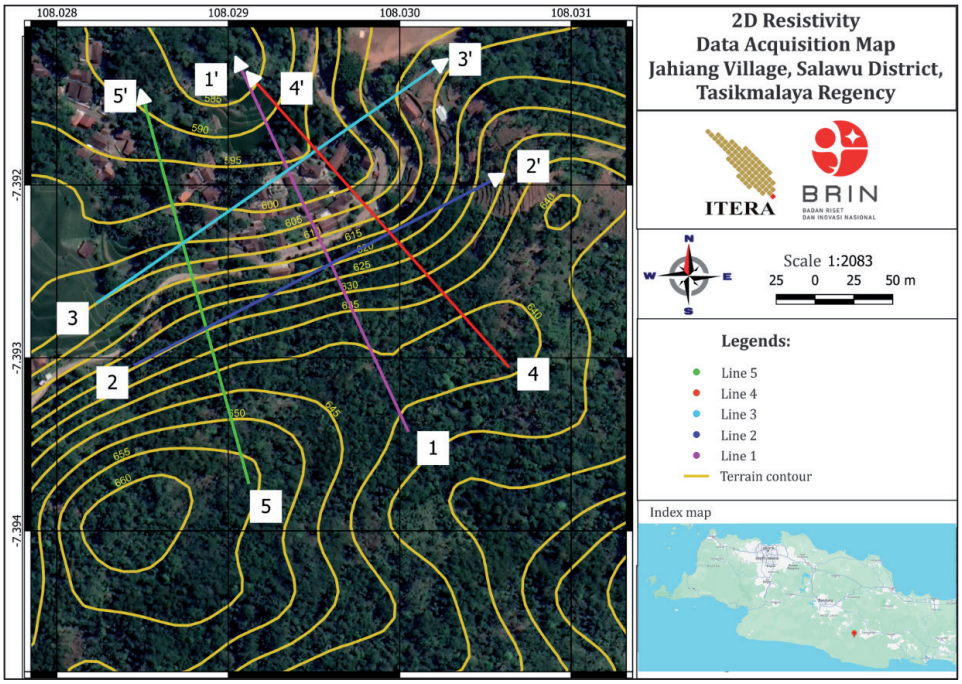

Figure 2. Data acquisition map of the study area. Line 1 – 5 are the survey lines.

METHODS

The resistivity geoelectric method is the study of the electrical resistance properties of rock layers in the earth. This method injects current (I) through two current electrodes (A and B). Then, the potential difference (ΔV) is measured through the other two electrodes (M and N), from which the variation in the type resistance value of each layer below the measuring point will be determined (Dentith & Mudge, 2014; Reynolds, 2011). The measured resistivity value is called the apparent resistivity (ρ_a), which is written using the following equation

$$\rho_a = K\left(\frac{\Delta V}{I}\right) \quad (1)$$

In the dipole-dipole configuration, the distance (a) between the current electrodes is the same as between the potential electrodes. The electrode distance multiplying factor (n) is implemented to obtain the distance between the current (A) and inner potential (M) electrodes (Figure 3). Variations in n are used to obtain specific depths. The greater the n, the greater the depth obtained. The level of range sensitivity in the dipole-dipole configuration is influenced by the magnitude of a and variations in n (Rachmawati et al., 2021). The imaging of the dipole-dipole configuration is comparable to the pole-dipole configuration. It is better than other configurations, especially in areas with vertical structures and steep slopes, but the depth resolution is not the best (Dahlin & Zhou, 2004). To calculate the value of the geometry factor (K) for the dipole-dipole can use the following equation,

$$K = \pi n a(n+1)(n+2) \quad (2)$$

(all units in the equations (1) and (2) are in the International System).

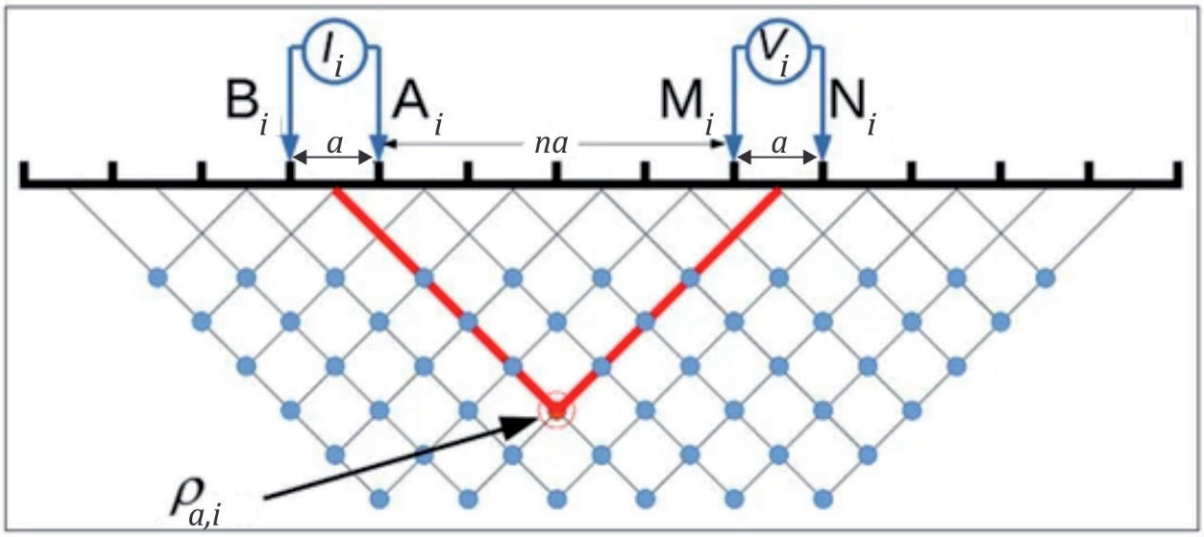

Figure 3. Dipole-dipole array illustration for the 2D resistivity method (modified from Cozzolino et al., 2022).

Figure 3 presents the measurement illustration of the dipole-dipole configuration in the 2D resistivity technique. The data in this study consisted of 5 straight lines with a spacing between electrodes of 5 m and a length of 275 m. Lines 1, 4, and 5 are in a southeast-northwest direction, while the others are in a southwest-northeast. The data acquisition design can be seen in Figure 2. With these lines, we expect to cover the slip plane analysis in the area as an initial assessment to mitigate the landslide.

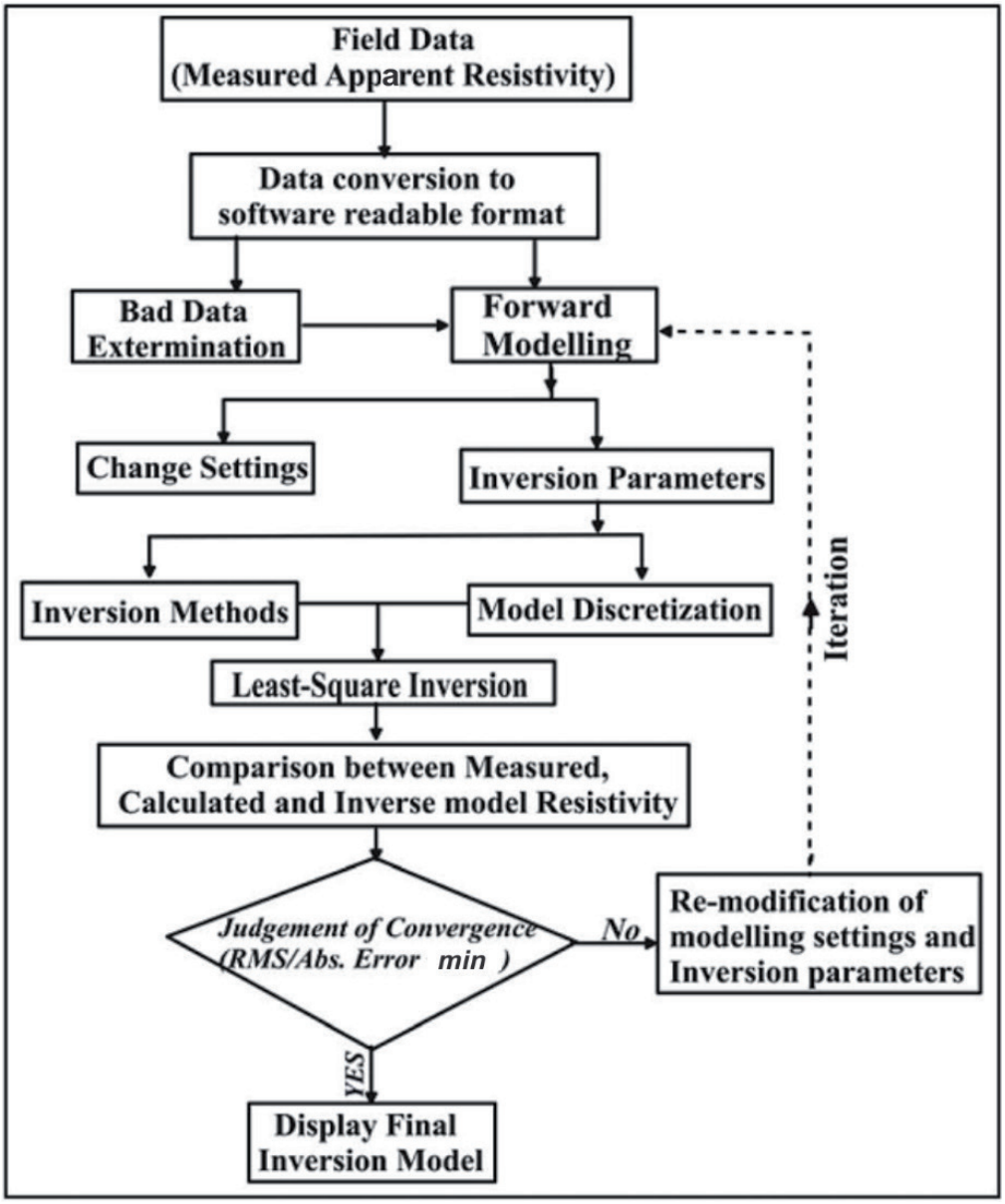

Figure 4. Flowchart of the Res2DInv software (Akingboye & Ogunyele, 2019).

Field measurements only produce apparent resistivity values, so inversion modeling must be carried out to approximate actual resistivity values. The observation data are expected to provide information about the physical properties of rocks and the condition and geometric location of subsurface anomalies. The relationship between the physical properties of the rock and the observation data, then, can be modeled mathematically based on physical parameters from observation data. We used Res2DInv for the 2D modeling. The outcome was the pseudosection model of the estimated actual resistivity in the subsurface. The software's step process can be viewed in Figure 4. In the inversion process, an iteration was performed to produce a minimum RMS error value. The number of iterations used in this study was ten times, which is commonly sufficient to get a minimum error. The error showed the level of match between calculated data and observation data. The more significant the RMS misfit value obtained, the more the 2D observed section would not match the computed data section and vice versa. The better the calculated data was fitted to the observation one, the more significant the subsurface 2D resistivity model was generated, which was then correlated with the geological map of Tasikmalaya, West Java (Figure 1).

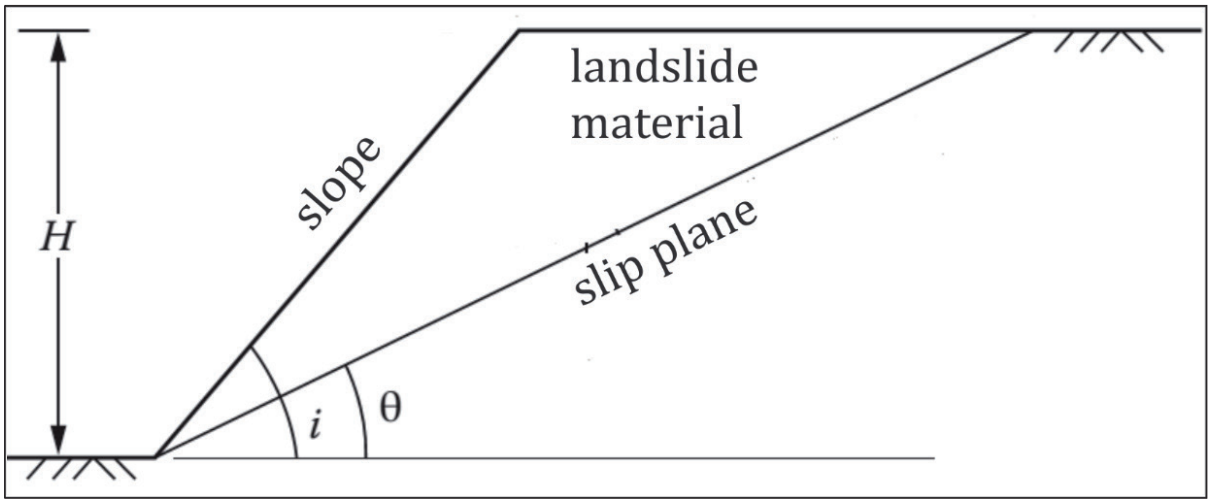

Figure 5. Slip plane diagram (modified from Sivakugan et al., 2013).

Afterward, the factor of safety (*FS*) was calculated manually from the interpreted resistivity pseudosection. The purpose was to assess the slope stability. According to Sivakugan et al. (2013), the *FS* computation refers to the Mohr-Coloumb failure criteria. It relates to the strength of the slip plane to withstand the mass at the top of the slip area. Its formula can be written as follows,

$$FS = \frac{2c \sin i}{\gamma H \sin\theta \sin(i-\theta)} + \frac{\tan\phi}{\tan\theta} \quad (3)$$

with,

γ = weight density (kN/m^3),

c = cohesion stress of the slip plane (kN/m^2),

H = height of the slip plane (m),

ϕ = friction angle of the slip plane (°),

i, θ = angle of the slope and the slip plane (°).

RESULTS AND DISCUSSION

The resistivity distribution in the study area ranges from 1.0 Ωm to more than 300 Ωm. Overall, the RMS error of the models is approximately 9% to 20%, resulting in the generated resistivity model being appropriately favorable. Lines 2 and 3 cross the other sections. Both have a similar topographic surface at the start of each line, almost flat, and the elevation is increasing at the end. The others also have an identical terrain from the beginning of the line, declining until the end of each line, although the first line does not seem too steep compared to lines 4 and 5. These outputs are shown in Figure 6.

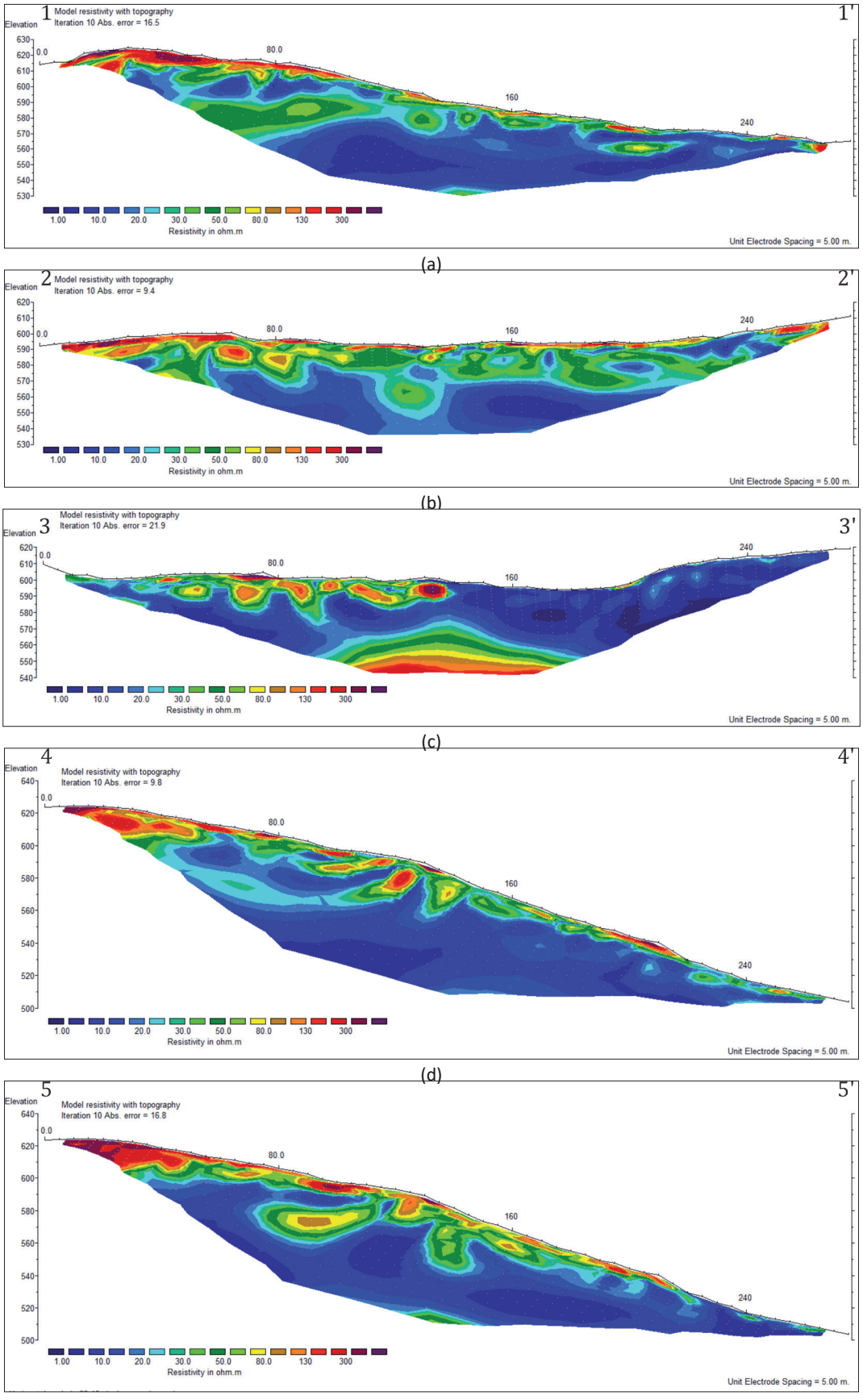

Figure 6. 2D resistivity distribution in the study area, (a) line 1, (b) line 2, (c) line 3, (d) line 4, and (e) line 5.

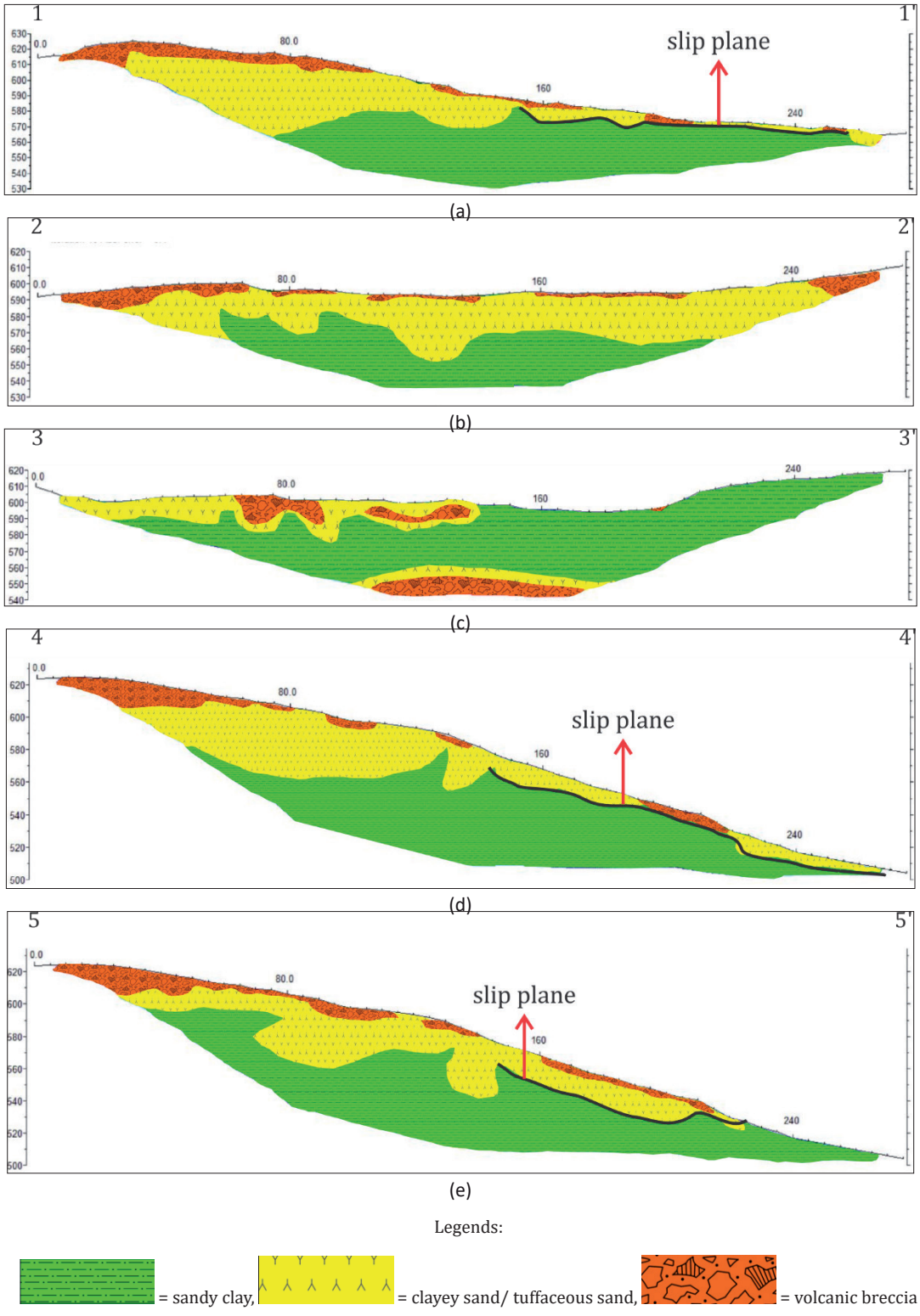

Figure 7. 2D rock model in the study area, (a) Line 1, (b) Line 2, (c) Line 3, (d) Line 4, and (e) Line 5.

According to Sarah & Daryono (2012), the rock type in the study location consists of sandy clay, clayey sand, and breccia. To define those rocks from the resistivity values in the 2D sections, we refer to Harja et al. (2023) and Widodo & Irawan (2019). Hence, the resistivity distribution of each layer is presented in Table 1. Then, the estimated rock profile of each pseudosection can be viewed in Figure 7. The slip plane from profiles 2 and 3 cannot be determined due to their relatively flat slopes. However,

the other profiles have a slip plane from the middle to the end of each line, and its direction is to the northwest. In this case, sandy clay is the layer that acts as a slip plane because of its impermeability characteristic. This sandy clay rock cannot pass water well, so water cannot flow to the layer below it but flows towards the slope, which can cause landslides. It has a depth of approximately 5 m to 10 m from the ground surface. The rocks above, which consists of clayey/tuffaceous sand and breccia, are the slipping mass. Clayey/tuffaceous sand has a better permeability than others in this study case (Table 2). Its mass would increase when saturated by rainwater. This event might cause the sandy clay's surface to become slippery. Then clayey/tuffaceous sand would slip, the breccia might be pushed to drop, and both would fall down the slope.

Regarding this analysis, the resistivity technique with the dipole-dipole configuration can delineate the high resistivity distribution associated with volcanic breccia. From the results, it has a boulder shape on each profile and a layered-like rock on the top of profiles 1, 4, and 5. This objective study of the dipole-dipole use is achieved. The breccia layer is in the near-surface. According to Table 2, this type of rock has the highest weight density and cohesion stress. These parameters mean that it has better compactness and rigidity than sandy clay and clayey sand. Hence, the presence of this breccia is significant since if it slips it would seriously damage the area affected by the landslide.

Table 1. Rock interpretation from resistivity value.

Resistivity (Ωm)	Rock type
< 25	Sandy clay
20-105	Clayey sand/ tuffaceous sand
> 80	Volcanic breccia

Table 2. Soil/ rock mechanics parameters (Sarah & Daryono, 2012).

Soil/ rock property	Sandy clay	Clayey sand	Volcanic breccia
γ (kN/m^3)	18	16,4	19
Permeability (m/day)	0.03	0.32	0.0026
θ (°)	12.00 – 21.30	13.00 – 25.98	35.00
c (kN/m^2)	6.00 – 21.74	6.00 – 12.50	150.00

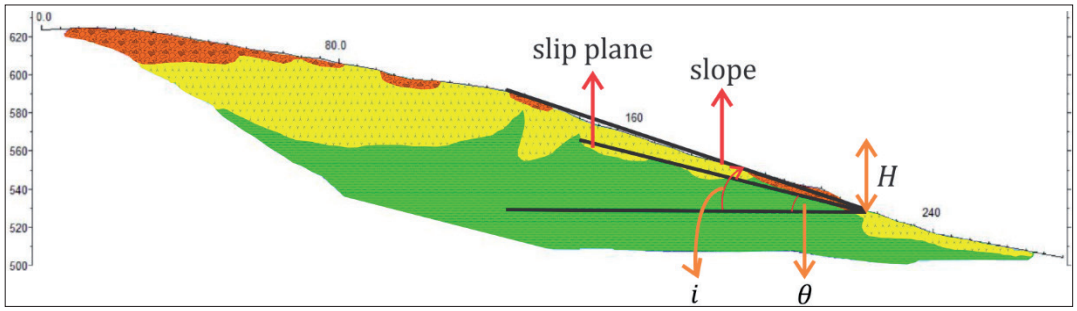

Figure 8. The simple assumption of slope and slip angles refers to Figure 5.

Based on the assumption of slope and slip angles (Figure 8), we calculated the Factor of Safety (*FS*) using Equation (3). Each section's slip and slope angles can be manually estimated from the three models in Figure 7 that indicate the slip plane. The first profile (Figure 7(a)) has a slope and slip angles of about 20° and 10°, respectively, with an estimated slip height of 20 m. Then, the fourth and last profiles (Figure 7(d-e)) have similar slope and slip values, approximately 40° for the hill and 33°-35° for the slip plane angle, with a slip height of about 40 m. We applied the soil and rock mechanics data

from Sarah & Daryono (2012), which is displayed in Table 2. The first line factor of safety is more than 1.35, and the other two (profiles 4 and 5) have a safety factor of 0.41-0.95. The results of referring to the Bowless criteria show that line 1 has a sound slope stability. Meanwhile, the slope in lines 4 and 5 is unstable, which means a landslide would happen if the rain falls frequently in the area.

The 3D presentation of the model (Figure 9) displays the slip area and the approximate landslide-prone zone. Figure 2 indicates that the profiles of lines 4 and 5 cross the residential area. That part of the area requires intensive attention from the local government and community to mitigate the disaster. While this study provides the possibility of a landslide occurring in the location, further comprehensive surveys for the in-situ geomechanical tests are required to confirm this study's analysis.

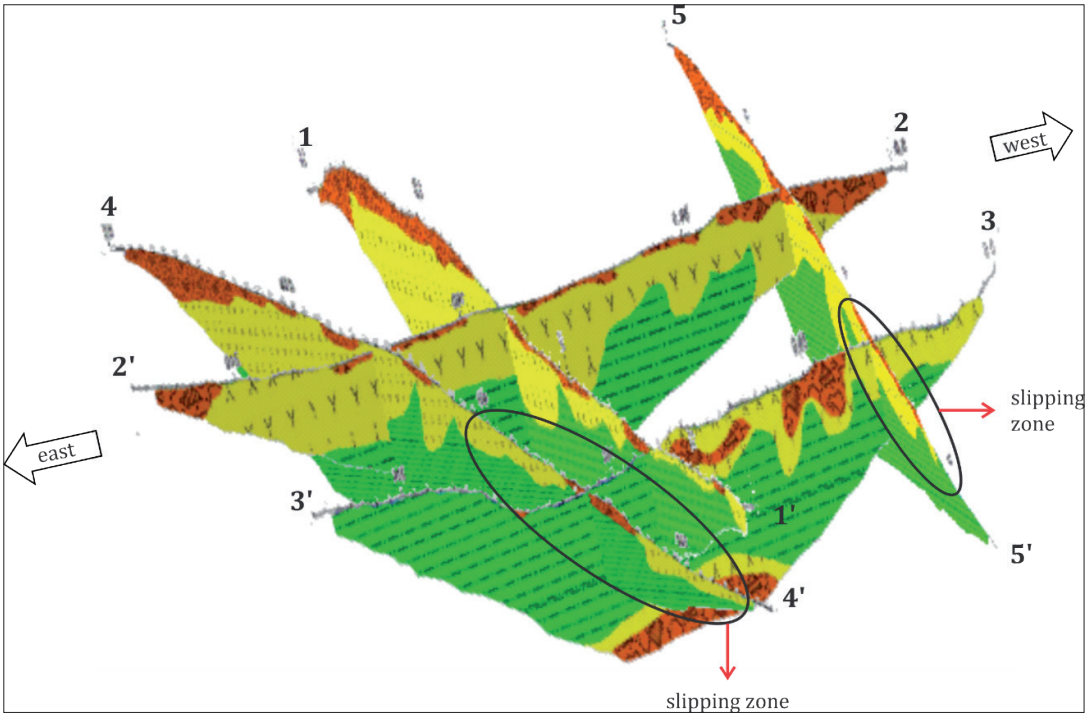

Figure 9. 3D cross-section visualization of all profiles.

CONCLUSION

The outcome of the 2D resistivity method is the resistivity distribution related to the geological rock profile. In general, the models indicate three classes of resistivity, which are low, medium, and high resistivity. The resistivity property is associated with permeability and compactness parameters. A value under 20 Ωm is considered a low resistivity, interpreted as sandy clay, which has medium permeability (impermeable) and minor to medium cohesion stress. The value of about 20-80 ΩΩm is defined as clayey sand. It has high permeability, eases water flow, and has minor to medium cohesion stress. This cohesion parameter of sandy clay and clayey sand explains that they can be quickly loose. A value above 80 ΩΩm is assigned to volcanic breccia, which has the highest cohesion value, far higher than that of other rocks. The breccia is physically almost massive and stiff, so it refers to a high resistivity. In contrast, it has a far smaller permeability value than the others, meaning it almost perfectly cannot absorb and flow the water. The breccia is described well in each profile in this study. This rock's layer would be hazardous when it becomes a slipping material when a landslide occurs. Furthermore, clayey/tuffaceous sand is the layer beneath the breccia, and the slip plane is sandy clay. There are spots with safety factor values under 1.00, which means that the slope in Jahiang Village, Salawu District, generally has weak stability. A subsequent study of in-situ soil/rock mechanics survey is required to confirm these results because some areas need intensive attention regarding the possibility of a landslide occurrence.

ACKNOWLEDGEMENT

The authors acknowledge the Research Center for Geological Disasters – National Research and Innovation Agency (BRIN) for the data support.

REFERENCES

Adi, A. W., Shalih, O., Shabrina, F. Z., Rizqi, A., Putra, A. S., Karimah, R., Eveline, F., Alfian, A., Syauqi, Septian, R. T., Widiastomo, Y., Bagaskoro, Y., Dewi, A. N., Rahmawati, I., Seniarwan, Suryaningrum, H. A., Purnamasiwi, D. I., & Puspasari, T. J. (2023). *IRBI Indeks Risiko Bencana Indonesia Tahun 2022* (R. Yunus, Ed.; Vol. 01). Badan Nasional Penanggulangan Bencana.

Akingboye, A. S., & Ogunyele, A. C. (2019). Insight into seismic refraction and electrical resistivity tomography techniques in subsurface investigations. *Rudarsko Geolosko Naftni Zbornik*, *34*(1), 93–111. https://doi.org/10.17794/rgn.2019.1.9

Al-Oufi, A., Al-Malabeh, A., & Al-Tarazi, E. (2012). Characterization of Lava Caves, Using 2D Induced Polarization Imaging, Umm Al Quttein area, NE Jordan. *15th International Symposium on Vucanospeleology*, 71–83. https://www.researchgate.net/publication/310599706

Analisa global. (2021). Longsor di Salawu, Putus Akses Jalan Penghubung Desa Sundawenang dan Desa Jahiang. *Analisa Global*. https://www.analisaglobal.com/longsor-di-salawu-putus-akses-jalan-penghubung-desa-sundawenang-dan-desa-jahiang/

Antosia, R. M. (2023a). The simple way to build a geoelectrical instrument. *ARPN Journal of Engineering and Applied Sciences*, *18*(04), 369–380. https://doi.org/10.59018/022357

Antosia, R. M., Akbar, H. H., Santoso, N. A., Putri, I. A., Farishi, B. Al, & Natalia, H. C. (2023b). Beneath the Surface: Identifying Subsurface Caves in "Gua Pandan" Using Integrated Electrical Profiling Method. *POSITRON*, *13*(1), 31–40. https://doi.org/10.26418/positron.v13i1.63558

Antosia, R. M., Akbar, H. H., Santoso, N. A., Putri, I. A., Farishi, B. A., & Natalia, H. C. (2023c). Underground-caves connectedness preview using the geoelectrical profiling method as an effort to revive natural tourism in "Gua Pandan," East Lampung Regency. *IOP Conference Series: Earth and Environmental Science*, *1173*(1). https://doi.org/10.1088/1755-1315/1173/1/012072

Antosia, R. M., & Ramdan, M. (2023d). A Combined Method of 1D and 2D Resistivity for Groundwater Layer Estimation at a Farming Area in Rejomulyo Village. *SPEKTRA: Jurnal Fisika Dan Aplikasinya*, *8*(1), 43–54. https://doi.org/10.21009/SPEKTRA

Arifin, M. H., Kayode, J. S., Izwan, M. K., Zaid, H. A. H., & Hussin, H. (2019). Data for the potential gold mineralization mapping with the applications of Electrical Resistivity Imaging and Induced Polarization geophysical surveys. *Data in Brief*, *22*, 830–835. https://doi.org/10.1016/j.dib.2018.12.086

Azwar, H. A. (2017). Longsor Tasikmalaya Timpa Rumah, 2 Orang Meninggal Dunia. *Portal Berita InfoPublik*. https://infopublik.id/read/225300/index.html

Budhitrisna, T. (2010). *Peta Geologi Lembar Tasikmalaya* (Edisi ketiga). Pusat Survei Geologi.

Cozzolino, M., Mauriello, P., & Patella, D. (2022). The Extended Data-Adaptive Probability-Based Electrical Resistivity Tomography Inversion Method (E-PERTI) for the Characterization of the Buried Ditch of the Ancient Egnazia (Puglia, Italy). *Applied Sciences (Switzerland)*, *12*(5). https://doi.org/10.3390/app12052690

Dahlin, T., & Zhou, B. (2004). A numerical comparison of 2D resistivity imaging with 10 electrode arrays. *Geophysical Prospecting*, *52*(5), 379–398. https://doi.org/10.1111/j.1365-2478.2004.00423.x

Darsono, D., Nurlaksito, B., & Legowo, B. (2012). Identifikasi Bidang Gelincir Pemicu Bencana Tanah Longsor Dengan Metode Resistivitas 2 Dimensi Di Desa Pablengan Kecamatan Matesih Kabupaten Karanganyar. *Indonesian Journal of Applied Physics*, *2*(02), 51–60.

Dentith, M., & Mudge, S. (2014). *Geophysics for the Mineral Exploration Geoscientist*. Cambridge University Press.

Dewi, K. K., Utama, W., & Rochman, J. P. G. N. (2017). Pemetaan Zona Korosivitas Tanah Berdasarkan Nilai Chargeability Menggunakan Metode Time Domain Induced Polarization Konfigurasi Dipole-Dipole Studi Kasus PT. IPMOMI. *Jurnal Geosaintek*, *3*(2), 137–142. https://doi.org/10.12962/j25023659.v3i2.2971

Djakamihardja, A. S. (2008). Geotechnical Investigation of Land Movement on Roadway at KM 23, Citatah Area, West Java Province. *Jurnal RISET Geologi Dan Pertambangan*, *18*(2), 41–50. https://doi.org/10.14203/risetgeotam2008.v18.15

Fatimah, F., Rizqi, A. H. F., & Yudhana, W. M. B. (2021). Aquifer Mapping Based on Stratigraphic and Geoelectrical Data Analysis in Bedoyo Region, Gunung Kidul Regency, Yogyakarta Special Region. *RISET Geologi Dan Pertambangan*, *31*(1), 13–26. https://doi.org/10.14203/risetgeotam2021.v31.1137

Harja, A., Aprilia, B. A., Susanto, K., & Fitriani, D. (2023). Identifikasi Zona Akuifer Menggunakan Metode Resistivitas-DC di Daerah Kipas Lava Pegunungan Malabar Kabupaten Bandung Jawa-Barat. *Jurnal Ilmu Dan Inovasi Fisika*, *7*(1), 49–57. https://doi.org/10.24198/jiif.v7i1.43216

Kompas. (2011). Gerakan Tanah Berpotensi Terjadi. *Kompas Gramedia Digital Group*. https://nasional.kompas.com/read/2011/08/19/12231191/~Regional~Jawa

Miranti, S. A. (2022). Ada 374 Bencana di Kabupaten Tasikmalaya selama 2022, Didominasi Tanah Longsor - Tribunjabar.id. *Tribun Jabar*. https://jabar.tribunnews.com/2022/12/29/ada-374-bencana-di-kabupaten-tasikmalaya-selama-2022-didominasi-tanah-longsor

Muslim, I. W. (2019). 6 Rumah dan Satu Masjid di Tasik Terancam Longsor. *Ayo Bandung*. https://www.ayobandung.com/regional/amp/pr-79647746/6

Putra, M. H. Z., Kartiko, R. D., Soemantidiredja, P., Sadisun, I. A., & Tohari, A. (2020). Pengaruh Zona Jenuh Air Terhadap Kestabilan Lereng di Weninggalih, Kabupaten Bandung Barat. *RISET Geologi Dan Pertambangan*, *30*(1), 119–130. https://doi.org/10.14203/risetgeotam2020.v30.1086

Rachmawati, S. K., Sudrajat, Y., Handayani, L., & Wardhana, D. D. (2021). Metode Geolistrik Konfigurasi Dipole-Dipole Untuk Penetapan Bidang Gelincir Gerakan Tanah di Jajaway, Palabuhanratu, Sukabumi. *Jurnal Lingkungan Dan Bencana Geologi*, *12*(1). https://doi.org/10.34126/jlbg.v12i1.354

Reynolds, J. M. (2011). *An Introduction to Applied and Environmental Geophysics* (2nd Edition). John Wiley & Sons, Ltd. www.wiley.com/go/reynolds/introduction2e

Sarah, D., & Daryono, M. R. (2012). Engineering Geological Investigation of Slow Moving Landslide in Jahiyang Village, Salawu, Tasikmalaya Regency. *Indonesian Journal of Geology*, *7*(1), 27–38.

Sivakugan, N., Shukla, S. K., & Das, B. M. (2013). *Rock Mechanics An Introduction*. CRC Press.

Stevanato, R., Ferreira, F. J. F., Canata, R. E., Mlenek, D. C., Leite, A. A., & Neto, D. N. (2019). Resistivity and induced polarization applied to "Buraco do Inferno" Cave, São Desidério, State of Bahia, Brazil. *Sixteenth International Congress of the Brazilian Geophysical Society*, 1–5. https://doi.org/10.22564/16cisbgf2019.270

Taufiqurrohman, R., Nugraha, D. M., & Bahri, A. S. (2017). Aplikasi Geolistrik 2D untuk Identifikasi Bidang Gelincir Studi Kasus Daerah Lereng Nglajo, Cepu. *Jurnal Geosaintek*, *3*(3), 155–160. https://doi.org/10.12962/j25023659.v3i3.3213

Van Bemmelen, R. W. (1949). *The Geology of Indonesia* (Vol. 1A). Government Printing Office.

Vargemezis, G., Fikos, I., & Tsourlos, P. I. (2015). Application of Electrical Resistivity Tomography Method to the Mapping of Explored Caves and Detection of Possible New Chambers: Case Studies from Greece. *8th Congress of the Balkan Geophysical Society, BGS 2015*. https://doi.org/10.3997/2214-4609.201414132

Wakhidah, N., Khumaedi, & Dwijananti, P. (2014). Identifikasi Pergerakan Tanah Dengan Aplikasi Metode Geolistrik Konfigurasi Wenner-Schlumberger Di Deliksari Gunungpati Semarang. *Unnes Physics Journal*, *3*(1), 1–6.

Widodo, A., & Irawan, P. (2019). Eksplorasi Air Tanah di Kampus Universitas Siliwangi dalam Rangka Pengelolaan Sumber Daya Air Berkelanjutan. *Jurnal Siliwangi*, *5*(2), 56–63.

Yuniardi, Y., Hendarmawan, H., Abdurrokhim, A., Isnaniawardhani, V., Mohammad, F., Alfadli, M. K., & Ridwan, P. (2019). Pendugaan Akifer Airtanah dengan Metode Geolistrik Konfigurasi Schlumberger di Lereng Utara Gunungapi Tangkubanparahu. *RISET Geologi Dan Pertambangan*, *29*(2), 239–253. https://doi.org/10.14203/risetgeotam2019.v29.1051